Coordination of plant hydraulic and photosynthetic traits: confronting optimality theory with field measurements

Article

Published Version

Creative Commons: Attribution-Noncommercial-No Derivative Works 4.0

Open Access

It is advisable to refer to the publisher's version if you intend to cite from the work. See Guidance on citing.

To link to this article DOI: http://dx.doi.org/10.1111/nph.17656

Publisher: Wiley

www.reading.ac.uk/centaur

CentAUR

Central Archive at the University of Reading

Reading's research outputs online

Coordination of plant hydraulic and photosynthetic traits: confronting optimality theory with field measurements

Huiying Xu[1,2] (iD), **Han Wang**[1,2] (iD), **I. Colin Prentice**[1,3,4] (iD), **Sandy P. Harrison**[1,5] (iD) and **Ian J. Wright**[4] (iD)

[1]Ministry of Education Key Laboratory for Earth System Modeling, Department of Earth System Science, Tsinghua University, Beijing 100084, China; [2]Joint Center for Global Change Studies (JCGCS), Beijing 100875, China; [3]Department of Life Sciences, Georgina Mace Centre for the Living Planet, Imperial College London, Silwood Park Campus, Buckhurst Road, Ascot, SL5 7PY, UK; [4]Department of Biological Sciences, Macquarie University, North Ryde, NSW 2109, Australia; [5]School of Archaeology, Geography and Environmental Sciences (SAGES), University of Reading, Reading, RG6 6AH, UK

Summary

- Close coupling between water loss and carbon dioxide uptake requires coordination of plant hydraulics and photosynthesis. However, there is still limited information on the quantitative relationships between hydraulic and photosynthetic traits.
- We propose a basis for these relationships based on optimality theory, and test its predictions by analysis of measurements on 107 species from 11 sites, distributed along a nearly 3000-m elevation gradient.
- Hydraulic and leaf economic traits were less plastic, and more closely associated with phylogeny, than photosynthetic traits. The two sets of traits were linked by the sapwood to leaf area ratio (Huber value, v_H). The observed coordination between v_H and sapwood hydraulic conductivity (K_S) and photosynthetic capacity (V_{cmax}) conformed to the proposed quantitative theory. Substantial hydraulic diversity was related to the trade-off between K_S and v_H. Leaf drought tolerance (inferred from turgor loss point, $-\Psi_{tlp}$) increased with wood density, but the trade-off between hydraulic efficiency (K_S) and $-\Psi_{tlp}$ was weak. Plant trait effects on v_H were dominated by variation in K_S, while effects of environment were dominated by variation in temperature.
- This research unifies hydraulics, photosynthesis and the leaf economics spectrum in a common theoretical framework, and suggests a route towards the integration of photosynthesis and hydraulics in land-surface models.

Introduction

Water transport is essential for plant survival and growth. Hydraulic failure triggers death under severe drought (Rowland *et al.*, 2015), and differences in hydraulic traits can be used to predict drought-induced tree mortality (Choat *et al.*, 2018). Photosynthesis is constrained by hydraulics because water transported through the xylem must replenish water lost through stomata during CO_2 uptake (Brodribb, 2009). Empirical studies (Brodribb *et al.*, 2007; Scoffoni *et al.*, 2016; Zhu *et al.*, 2018) and optimality arguments (Deans *et al.*, 2020) support a tight coordination between hydraulic and photosynthetic traits. Nonetheless, quantitative understanding of their relationships remains incomplete (Mencuccini *et al.*, 2019b). Embedding plant hydraulics in vegetation and land-surface models is desirable (Christoffersen *et al.*, 2016; Mencuccini *et al.*, 2019a), not least because an improved understanding of drought effects on photosynthesis and transpiration could remove a leading source of uncertainty in global models (De Kauwe *et al.*, 2015). This situation provides a strong motivation for theoretical and empirical research on how whole-plant hydraulic traits are related to (better studied) leaf photosynthetic traits.

The ratio of sapwood area to subtended leaf area (the Huber value, v_H) links whole-plant to leaf processes (Mencuccini *et al.*, 2019b; Rosas *et al.*, 2019). There is a limit to the amount of leaves that a given area of sapwood can support due to its limited capacity to supply water. The plant needs to invest more carbon in sapwood to meet increasing water loss, or to shed leaves to decrease water loss. Therefore, v_H reflects not only the balance between water supply and loss, but also carbon allocation to stems versus leaves. Plants with low v_H tend to have low leaf mass per area (LMA) and low leaf stable carbon isotope ratios ($\delta^{13}C$), implying a high ratio of leaf-internal to ambient CO_2 (χ); high maximum CO_2 assimilation rate (A_{sat}); high leaf water potential at the turgor loss point (Ψ_{tlp}, a negative quantity); and high sapwood-specific hydraulic conductivity (K_S) (Zhu *et al.*, 2018; Mencuccini *et al.*, 2019b; Rosas *et al.*, 2019). High V_{cmax} and high LMA both require (all else equal) a high v_H, the former because high V_{cmax} is associated with high photosynthetic rate,

stomatal conductance and transpiration, the latter because high-LMA leaves tend to be associated with low hydraulic conductance. There is considerable independent variation in V_{cmax} (expressed on an area basis) and LMA that implies that these are separate dimensions influencing v_H. Previous studies have also shown that hydraulic traits are influenced by environmental variables, particularly aridity (Martinez-Vilalta *et al.*, 2009; Gleason *et al.*, 2013; Togashi *et al.*, 2015; Liu *et al.*, 2019), in a coordinated way. Drought-adapted plants are characterised by reduced water supply through stems (low hydraulic efficiency, K_S; for example associated with narrow conduits) and/or reduced demand (high v_H), and increased leaf hydraulic safety (low Ψ_{tlp}). Photosynthetic and leaf economic traits are also influenced by climate. χ increases with growth temperature, and decreases with vapour pressure deficit (D) and elevation (Prentice *et al.*, 2014; Wang *et al.*, 2017). Photosynthetic capacity (maximum RuBisCo carboxylation rate, V_{cmax}) increases with light, and weakly with temperature and D (Smith *et al.*, 2019). LMA increases with light and aridity, and decreases with temperature (Wright *et al.*, 2004; Poorter *et al.*, 2009). Although these traits show strong trends with climate, phylogeny controls the variation of hydraulic traits to a large extent due to their dependence on conservative characteristics such as wood anatomy (Rosas *et al.*, 2019), while photosynthesis-related traits regulated by biochemical processes show a high degree of plasticity (Dong *et al.*, 2020).

Optimality theory allows testable predictions about trait–trait coordination and can also provide strong explanations for observed responses of traits to environment (Franklin *et al.*, 2020). Among photosynthetic traits, analyses of $\delta^{13}C$ data have shown quantitative agreement between observed and theoretically predicted environmental responses of χ (Prentice *et al.*, 2014; Wang *et al.*, 2017; Lavergne *et al.*, 2020a). Smith *et al.* (2019), similarly, used optimality theory to predict the observed environmental responses of V_{cmax} in a global data set. Sperry *et al.* (2017) integrated hydraulic traits with a photosynthesis model to predict stomatal conductance using optimality theory. Less attention has been paid to applying optimality theory to predict leaf economic or hydraulic traits. Here we investigated the relationships among photosynthetic, leaf economic and hydraulic traits, and between these traits and climate, using field data collected from 11 sites in the Gongga Mountain region of western China. We extend the optimality framework of Prentice *et al.* (2014) and Wang *et al.* (2017), which hypothesises that plants minimise the total cost of maintaining the capacities for photosynthesis and water transport relative to photosynthesis rate, to make explicit quantitative predictions of these relationships. K_S and V_{cmax} are two key traits related to water transport and photosynthesis/water demand, respectively. Based on the requirement that water transport through xylem must equal water loss via stomata, our optimality model indicates a key role for v_H in achieving this requirement (Mencuccini *et al.*, 2019b), and confirms a positive relationship between v_H and V_{cmax} but a negative one with K_S theoretically in a unified framework. Our model therefore provides a new theoretical basis to understand the variations of v_H along environmental gradients.

To test the model, we measured photosynthetic and hydraulic traits on 107 species at 11 sites located in the Gongga Mountain region of Sichuan Province, China. This region (Supporting Information Fig. S1) extends from 29°22′ to 29°55′N and 101°1′ to 102°9′E and spans an elevation range from near sea level to 8000 m, creating a long gradient in growing-season temperature. Sites from the western side of Gongga Mountain also tend to be drier than sites at corresponding elevations on the eastern side. By sampling 11 sites over a range of nearly 3000 m in elevation, from both the western and eastern sides, we assembled a data set on woody plants encompassing a wide range of climates.

Description

Theory

The theory of v_H variation extends the least-cost hypothesis of Prentice *et al.* (2014). According to Fick's law and Darcy's law respectively (Fick, 1855; Whitehead, 1998), transpiration can be calculated from either water demand (Eqn 1) or supply (Eqn 2). The coordination of xylem water transport and stomatal water loss implies that plants should optimally allocate resources so that maximum water transport matches maximum photosynthesis, which leads to Eqn 3:

$$E = 1.6g_s D/P_{atm} \qquad \text{Eqn 1}$$

$$E = K_S \Delta\Psi v_H/h \qquad \text{Eqn 2}$$

$$1.6g_s D/P_{atm} = K_S \Delta\Psi_{max} v_H/h \qquad \text{Eqn 3}$$

where E is the transpiration rate (mol m^{-2} s^{-1}), g_s is stomatal conductance to CO_2 (mol m^{-2} s^{-1}), D is the vapour pressure deficit (Pa) and P_{atm} is the atmospheric pressure (Pa). Here h is the path length (m), roughly equivalent to plant height; K_S is the sapwood-specific hydraulic conductivity (mol m^{-1} s^{-1} Pa^{-1}); v_H is the ratio of sapwood to leaf area (m^2 m^{-2}); $\Delta\Psi$ is the difference between leaf and soil water potential and $\Delta\Psi_{max}$ is the maximum decrease in water potential from soil to leaves (Ψ_{min} and Ψ_{soil}, Pa).

From the diffusion equation and the photosynthesis model of Farquhar, von Caemmerer and Berry (Farquhar *et al.*, 1980), we can calculate g_s from V_{cmax}, χ and m_C:

$$g_s = A/[(c_a/P_{atm})(1-\chi)] \qquad \text{Eqn 4}$$

$$A = m_C V_{c\,max} \qquad \text{Eqn 5}$$

$$m_C = (\chi c_a - \Gamma^*)/(\chi c_a + K) \qquad \text{Eqn 6}$$

where A is the assimilation (photosynthesis) rate (mol m^{-2} s^{-1}), c_a is the ambient partial pressure of CO_2 (Pa), χ is the ratio of leaf-internal to ambient CO_2 partial pressure (Pa Pa^{-1}), V_{cmax} is the maximum capacity of carboxylation (mol m^{-2} s^{-1}), Γ^* is the photorespiratory compensation point (Pa), and K is the effective Michaelis–Menten coefficient of RuBisCo (Pa). The factor m_C

reduces photosynthesis under natural conditions relative to V_{cmax}. Substituting g_s from Eqns 4–6 into Eqn 3 yields Eqn 7, which represents our key optimality theory linking hydraulic and photosynthetic traits. It states that maximum rate of water transport through the xylem equals the maximum rate of water loss through the stomata:

$$(K_S/h)v_H\Delta\Psi_{max} = 1.6(D/c_a)m_C V_{cmax}/(1-\chi) \qquad \text{Eqn 7}$$

As V_{cmax} acclimates to the environment on a weekly to monthly timescale, while K_S is determined by xylem structure and therefore less able to vary seasonally, we worked with V_{cmax} at the mean daily maximum temperature in July ($V_{cmax,jt}$) and K_S at the mean daily maximum temperature during the growing season (defined as the period with daytime temperatures > 0°C) ($K_{S,gt}$).

In practice, effects of K_S and h are not separable, because the tip-to-base widening of xylem elements implies a positive correlation between them that greatly reduces the effect of path length on whole-stem conductance, so that the whole-stem conductance is similar to or only slightly lower than the conductance measured near the branch tip (Christoffersen et al., 2016; Mencuccini et al., 2019b; Olson et al., 2021). We assume $\Delta\Psi_{max}$ to be equal to $-\Psi_{tlp}$ ($\Psi_{soil} \approx 0$ under well watered conditions) as Ψ_{tlp} is a proxy for Ψ_{min} (Hochberg et al., 2018). The uncertainty of the Ψ_{tlp} proxy has little effect on our results as it is not a principal predictor in our model (shown in Fig. 3). Therefore, to test Eqn 7 we take $-\Psi_{tlp}$ as a surrogate for $\Delta\Psi_{max}$ (Hochberg et al., 2018) and subsume the effect of height in a composite constant (C), leading to the following relationship after $\log_e$ transformation of Eqn 7:

$$\log_e(v_H) = \log_e(D) + \log_e(m_C) + \log_e(V_{cmax,jt}) - \log_e(K_{S,gt})$$
$$- \log_e(-\Psi_{tlp}) - \log_e(1-\chi) - \log_e(c_a) + C \qquad \text{Eqn 8}$$

where C has a fitted value of 2.27 using all the species sampled (see Fig. S4), which suggests an average 'effective tree height' of 6 m.

Photosynthetic traits can be estimated from existing optimality models. The least-cost hypothesis states that plants minimise the combined unit costs (that is, costs per unit of carbon assimilated) of maintaining the capacities for carbon fixation and water transport (Prentice et al., 2014). The coordination hypothesis states that light-limited and RuBisCo-limited photosynthesis rates are approximately equal, to be able to utilise the available light while avoiding wasteful maintenance costs (Chen et al., 1993). These two hypotheses have already been corroborated by many studies at regional or global scale (Smith et al., 2019; Lavergne et al., 2020b; Xu et al., 2021). χ in Eqn 8 can be estimated as follows, based on the least-cost hypothesis (Wang et al., 2017):

$$\chi = \Gamma^*/c_a + \xi(1 - \Gamma^*/c_a)/(\xi + \sqrt{D}) \qquad \text{Eqn 9}$$

where

$$\xi = \sqrt{[\beta(K + \Gamma^*)/(1.6\eta^*)]} \qquad \text{Eqn 10}$$

where β is the ratio at 25°C of the unit costs of maintaining carboxylation and transpiration capacities (146, based on a global compilation of leaf $\delta^{13}C$ measurements), η^* is the viscosity of water relative to its value at 25°C, and ξ (Pa$^{1/2}$) is a stomatal sensitivity parameter that increases with temperature due to the temperature dependencies of K, Γ^* (increasing) and η^* (decreasing).

$V_{cmax,jt}$ can also be predicted from climate, based on the coordination hypothesis (Smith et al., 2019):

$$V_{cmax,jt} \approx \phi_0 I_{abs}(c_i + K)/(c_i + 2\Gamma^*) \qquad \text{Eqn 11}$$

where ϕ_0 is the intrinsic quantum efficiency of photosynthesis (to which we assign the value 0.085 μmol C μmol^{-1} photon), I_{abs} is the photosynthetic photon flux density (PPFD) absorbed by leaves (mol m^{-2} s^{-1}), and c_i is the leaf-internal CO_2 partial pressure ($c_i = \chi c_a$) (Pa).

Data and methods

Trait data Trait data were measured at 11 sites in late July 2018 and August 2019, during the active growing season, in the Gongga Mountain region (29°34′16″–29°54′52″N and 101°59′08″–102°9′42″E, Fig. S1). We collected the data needed to allow the calculation of four leaf traits: leaf mass per area (LMA), leaf nitrogen per unit area (N_{area}), the maximum capacity of carboxylation (V_{cmax}), and the ratio of leaf-internal to ambient CO_2 partial pressure (χ). Hydraulic traits, specifically the ratio of sapwood to leaf area (Huber value, v_H), sapwood-specific hydraulic conductivity (K_S), wood density (WD) and leaf potential at turgor loss point (Ψ_{tlp}), were measured on all the woody broad-leaved species. We sampled all the tree species and at least five shrub species at each site. All samples were taken from the top canopy layer receiving direct sunshine.

LMA was calculated from the measurements of leaf area and dry weight following standard protocols (Cornelissen et al., 2003). Multiple leaves, or leaflets for compound leaves, were randomly selected and scanned using a Canon LiDE 220 Scanner. The dry weights of these leaves were measured after oven drying at 75°C for 48 h to constant weight. We calculated LMA as the ratio of dry mass to leaf area. Leaf nitrogen content was measured using an isotope ratio mass spectrometer (Thermo Fisher Scientific Inc., Carlsbad, CA, USA). N_{area} was calculated from LMA and leaf nitrogen content. The LMA value for a species at a given site was the average of three separate measurements made on leaves from multiple individuals, while N_{area} measurements were made on pooled samples of leaves from multiple individuals.

Carbon isotopic values ($\delta^{13}C$) were measured using an isotope ratio mass spectrometer (Thermo Fisher Scientific Inc.). Values were measured on pooled samples of leaves from multiple individuals. Estimates of χ were made using the method of Cornwell et al. (2018) to calculate isotopic discrimination (Δ) from $\delta^{13}C$ with a standard formula using the recommended values of d and b' of 4.4‰ and 27‰, respectively (Farquhar et al., 1989; Cernusak et al., 2013):

$$\chi = (\Delta - d')/(b' - d') \qquad \text{Eqn 12}$$

Leaf gas-exchange measurements were made in the field using a portable infrared gas analyser (IRGA) system (LI-6400; Li-Cor Inc., Lincoln, NB, USA). Sunlit branches from the outer canopy were collected and re-cut under water immediately before measurement. *In situ* measurements were taken with relative humidity and chamber block temperature similar to the ambient conditions, and a constant airflow rate (500 μmol s^{-1}). V_{cmax} at leaf temperature ($V_{cmax,lt}$) was calculated from the light-saturated rate of net CO_2 fixation at ambient CO_2, measured on one individual of each species, using the one-point method (De Kauwe *et al.*, 2016) and adjusted to a standard temperature of 25°C (V_{cmax25}) and maximum temperature in July ($V_{cmax,jt}$) using the method of Bernacchi *et al.* (2001).

Branches with a diameter wider than 7 mm were sampled for hydraulic traits. We cut the branch as close to the bifurcation point as possible, to minimise any effect of the measurement location on the measured area. We measured the cross-sectional area of the xylem at both ends of the short piece re-cut from the bottom of the branch using digital callipers. Sapwood area was calculated as the average of these two measurements. All leaves attached to the branch were removed and dried at 70°C for 72 h before weighing. The total leaf area was obtained from dry mass and LMA. The ratio of sapwood area and leaf area was calculated as v_H. The v_H value of one species at each site was the average of three measurements made on branches from different individuals.

Five branches from at least three mature individuals of the same species at each site were collected, wrapped in moist towels and sealed in black plastic bags, and then immediately transported to the laboratory. All the samples were re-cut under water, put into water and sealed in black plastic bags to rehydrate overnight. K_S was measured using the method described in Sperry *et al.* (1988). Segments (10–15 cm length) were cut from the rehydrated branches and flushed using 20 mmol l^{-1} KCl solution for at least 30 min (to remove air from the vessels) until constant fluid dripped from the segment section. The segments were then placed under 0.005 MPa pressure to record the time (t) they took to transport a known water volume (W, m^3). Length (L, m), sapwood areas of both ends (S_1 and S_2, m^2) and temperature (T_m, °C) were recorded. Sapwood-specific hydraulic conductivity at measurement temperature ($K_{S,m}$, mol m^{-1} s^{-1} MPa^{-1}) was calculated using Eqn 13. This was transformed to K_S at mean maximum temperature during the growing season ($K_{S,gt}$) and standard temperature (K_{S25}) following Eqns 14 and 15:

$$K_{S,m} = \{W L \rho_w / [0.005t(S_1 + S_2)/2]\}(1000/18) \qquad \text{Eqn 13}$$

$$K_{S,t} = K_{S,m} \eta_m / \eta_t \qquad \text{Eqn 14}$$

$$\eta = 10^{-3} \exp[A + B/(C + T)] \qquad \text{Eqn 15}$$

where η_m and η_t (Pa s) are the water viscosity at measurement temperature and transformed temperature (i.e. mean maximum daytime temperature during the growing season and standard temperature, 25°C in this study), respectively, and ρ_w (kg m^{-3}) is the density of water. The parameter values adopted in Eqn 15 were $A = -3.719$, $B = 580$ and $C = -138$ (Vogel, 1921).

A small part of each sapwood segment was used to measure WD, the ratio of dry weight to volume of sapwood. After removal of bark and heartwood, the displacement method was used to measure the volume of sapwood and the dry weight of sapwood was obtained after drying at 70°C for 72 h to constant weight. WD was calculated as the ratio of dry weight to the volume of sapwood.

We applied the method described by Bartlett *et al.* (2012) for the rapid determination of Ψ_{tlp}. After rehydration overnight, discs were sampled from mature, healthy leaves collected on each branch, avoiding major and minor veins and using a 6-mm-diameter punch. Leaf discs wrapped in foil were frozen in liquid nitrogen for at least 2 min and then punctured 20 times quickly with sharp-tipped tweezers. Five repeat experiments using leaves from multiple individuals were carried out for every species at each site. We measured osmotic potential (Ψ_{osm}) with a VAPRO 5600 vapour pressure osmometer (Wescor, Logan, UT, USA) and calculated Ψ_{tlp} (in MPa) as:

$$\Psi_{tlp} = 0.832\Psi_{osm} - 0.631 \qquad \text{Eqn 16}$$

Climate data We derived climate variables at each of the 11 sampled sites using meteorological data (monthly maximum and minimum temperature, fraction of sunshine hours and water vapour pressure) from 17 weather stations in the Gongga region (http://data.cma.cn/data/cdcdetail/dataCode/SURF_CLI_CHN_MUL_MON.html) and the elevation-sensitive ANUSPLIN interpolation scheme (Hutchinson & Xu, 2004). The meteorological data were available from January 2017 to December 2019. The monthly data were converted to daily values by linear interpolation to calculate the bioclimatic variables mean maximum temperature during the growing season (defined as the period with daytime temperature > 0°C), growing-season mean PPFD and vapour pressure deficit under maximum daytime temperature in July, using the Simple Process-Led Algorithms for Simulating Habitats (SPLASH) model (Davis *et al.*, 2017).

Data analysis All statistical analyses were carried out in R v.3.1.3 (R Core Team, 2015). To homogenise the variance, traits were log$_e$ transformed and χ was logit transformed; for Ψ_{tlp}, the absolute value ($-\Psi_{tlp}$) was log$_e$ transformed. Trait variance partitioning was carried out using the VEGAN package (Oksanen *et al.*, 2017) to quantify the amount of variation explained by different groups of factors. In this study, the groups are families (representing phylogenetic relatedness), life forms, climate and sites. Path analysis was used to characterise the trait coordination framework built on the idea that plastic traits are influenced by structural traits, using the LAVAAN package (Rosseel, 2012). The model was evaluated using the ratio of χ^2 and degree of freedom (χ^2/df) and goodness-of-fit index (GFI). The χ^2/df of models using all species and only evergreen species were below 3, and the GFI values of all three models were larger than 0.9 (Fig. 2). Traits under standard conditions (V_{cmax25} and K_{S25}) were used in variance partitioning, path analysis and bivariate regressions to eliminate the effect of

temperature, while trait values under growth conditions were used for theoretical prediction.

To examine the importance of each predictor in Eqn 8 for the prediction of v_H, we evaluated the contributions of each variable in four steps as follows. We analysed the contributions to variation in v_H using two sets of predictors: (1) the traits and environmental variables in Eqn 8 (D, K_S, Ψ_{tlp}, V_{cmax}, χ, c_a), with the contribution of the integrative predictor m_C included in the effects of χ and c_a; and (2) the hydraulic traits (K_S, Ψ_{tlp}) and environmental predictors (D, temperature, radiation, elevation) that influence v_H indirectly through their influence on photosynthesis-related traits. First the baseline value of each predictor was defined as the median of its site mean values across the 11 sites. These baseline values were used to generate baseline, a predicted value of $\log_e(v_H)$. Second, each predictor in turn was changed to its actual values at each site, while other predictors were kept at their baseline values. We used these inputs to calculate values of $\log_e(v_H)$ representing v_H variation across sites induced by this predictor alone. Third, the contribution of each predictor at each site was calculated as the difference between simulated $\log_e(v_H)$ values from the second and first steps (indicated as $\Delta\log_e(v_H)$ in Fig. 3). Last, we calculated the improvement in R^2 of the relationships between predicted $\log_e(v_H)$ and contributions of each predictor across sites. R^2 improvements due to each variable were averaged over orderings among predictors, yielding the relative importance of each variable. This procedure was run using the RELAIMPO package (Groemping, 2006). The partial residual plots from the regression model of the second set of predictors were plotted using the VISREG package (Breheny & Burchett, 2017) to better understand the environmental effects on v_H variation.

To assess the predictive power of the model, we used Deming regression of site mean predicted versus observed $\log_e(v_H)$ with its corresponding standard deviation (SD). The SD of predictions came from the observed variations of sapwood-specific hydraulic conductivity (K_S) and leaf water potential at turgor loss point (Ψ_{tlp}). Root mean square error (rmse) was estimated between the observed and predicted values both across sites and species. The Deming regression and rmse were calculated using the DEMING and XXIRT packages respectively.

Results

The measured traits can be ranked by phylogenetic influence, according to the fraction of variation explained by family alone in a variation partitioning analysis (Fig. 1). The hydraulic traits WD and sapwood-specific hydraulic conductivity at 25°C (K_{S25}) were most influenced by phylogeny (49–52%); LMA, leaf nitrogen per unit area (N_{area}) and Ψ_{tlp} were intermediate (28–31%); photosynthetic traits (χ and V_{cmax} at 25°C, V_{cmax25}) and v_H were least influenced by phylogeny (19–24%). These rankings are approximately mirrored by the percentages of variation explained by site factors and climate (Fig. 1).

Path analysis (Fig. 2) was used to test a framework for trait coordination, based on the hypothesis that the traits that are structurally dependent and more phylogenetically influenced

impose a constraint on more plastic traits, with v_H as the key trait linking the two sets of traits. Analyses conducted separately on evergreen and deciduous woody plants revealed several general patterns. First, v_H decreased with K_{S25}, but increased with V_{cmax25} (especially in evergreen plants) (Fig. 2). K_{S25} was also lower, and v_H higher, in plants with high LMA. The leaf economics spectrum (from low to high LMA: Wright et al. (2004)) therefore also influenced v_H, both directly and indirectly through K_{S25}. Second, WD was negatively related to K_{S25} (especially in deciduous plants), and positively related to $-\Psi_{tlp}$. Third, both LMA and $-\Psi_{tlp}$ negatively influenced χ. In other words, plants with low (more negative) turgor loss point and/or high LMA tended to operate with low χ, with low χ in turn being linked to higher V_{cmax} and therefore higher v_H. Fourth, N_{area} was found to depend jointly on LMA and V_{cmax25}, consistent with accumulating evidence – for example Dong et al. (2017), Xu et al. (2021) – for the dependence of N_{area} on leaf structure (with LMA as the dominant control, here as in other analyses), and a weaker relationship to V_{cmax25}. Together, through direct and indirect effects, these hypothesised causal pathways accounted for all of the significant bivariate relationship among traits (Fig. S2; Table S1).

Our analyses (Figs 2, S2) indicated only a weak trade-off between leaf drought tolerance and xylem hydraulic efficiency. K_{S25} and $-\Psi_{tlp}$ were negatively related for deciduous species, but this relationship was not significant for evergreen species, or across all species considered together.

The theoretical model, including just a single fitted parameter across all species (the intercept, reflecting the implicit effect of height), captured the essential trade-off between v_H and K_S. Both quantities v_H and K_S varied greatly among species (variance of $\log_e$-transformed variables = 0.4 and 0.73, respectively, averaged across the deciduous and evergreen species-sets; Table S1), allowing a wide variety of hydraulic strategies to coexist within communities. V_{cmax25} also varied widely among species (0.69), and more so than either χ (0.28) or Ψ_{tlp} (0.03) (Table S1). The model also predicted a tendency for plants with high V_{cmax} to have large v_H, and/or K_S, to allow a correspondingly high rate of water loss. This prediction was consistent with the partial residual plots based on the data (Figs 2, S3). Relationships between A_{sat} and plant hydraulic traits found in many studies (Santiago et al., 2004; Zhu et al., 2018) were consistent with this prediction. Moreover, Eqn 8 predicted environmental modulation of the relationship between v_H and other traits. Specifically, it predicted a positive impact of vapour pressure deficit (D) on v_H. As D increases, plants are therefore expected to allocate relatively less carbon to leaves, and more to stems and roots, resulting in increasing v_H. Temperature was another essential climate variable affecting v_H variation through χ and m_C with contrasting effects (positive on χ, but negative on m_C). Partial residual plots showed a net negative effect of temperature on v_H (Fig. S4a). However, elevation contributed little to v_H variation (Fig. 3b).

Predicted v_H captured 90% of the observed variation in v_H across sites (Fig. 4) and 20% across all species (Fig. S4). These predictions (see Eqn 8) were based on observed hydraulic traits and c_a, and on predicted optimal values of V_{cmax}, m_C and χ.
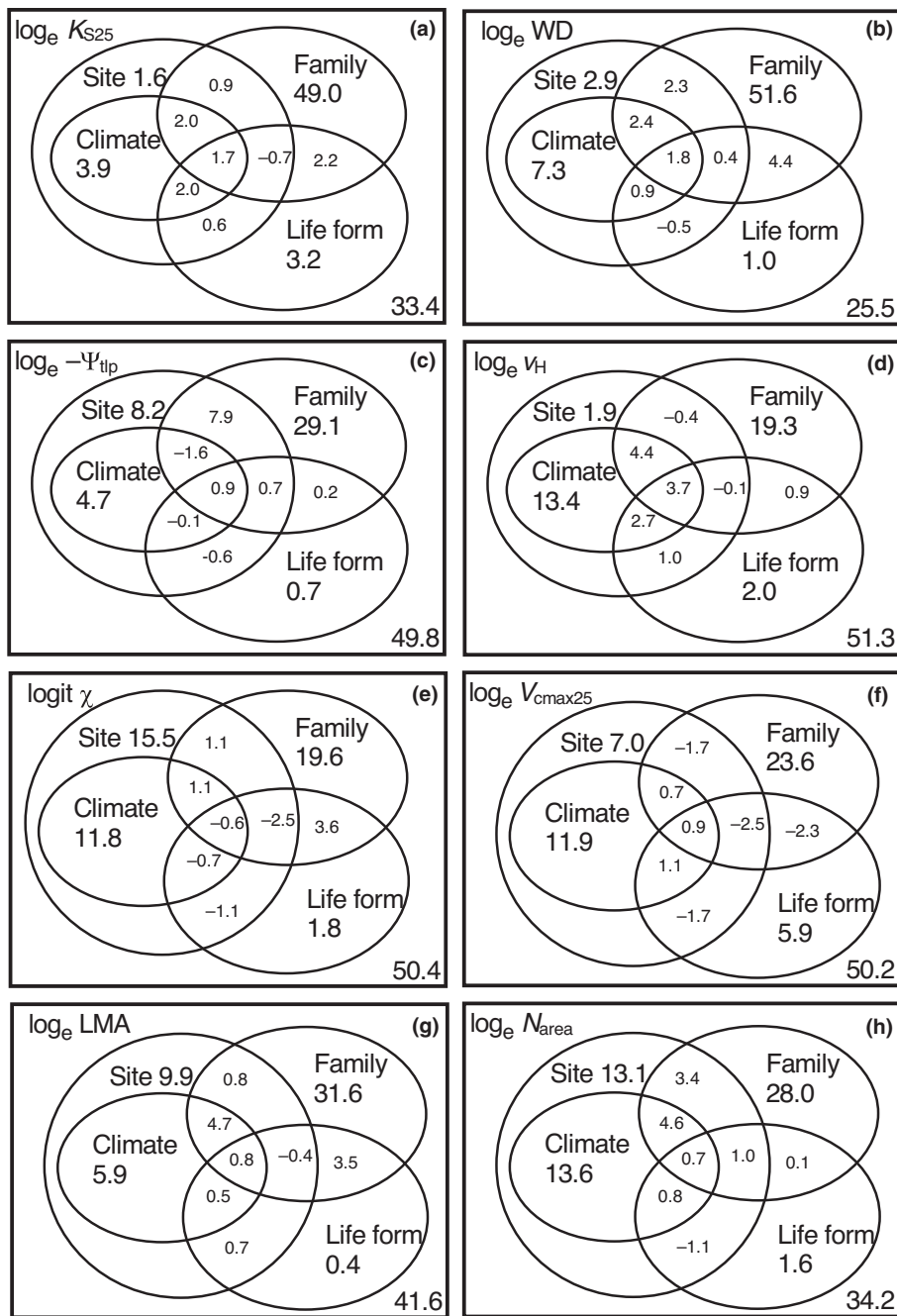
Fig. 1 Variance partitioning (%) for each trait. (a) K_{S25} is sapwood-specific hydraulic conductivity at 25°C, (b) WD is wood density, (c) Ψ_{tlp} is leaf water potential at turgor loss point, (d) ν_H is the ratio of sapwood to leaf area, (e) χ is the ratio of leaf-internal to ambient CO_2 partial pressure, (f) V_{cmax25} is the maximum capacity of carboxylation at 25°C, (g) LMA is leaf mass per area, and (h) N_{area} is leaf nitrogen content per area.

Analysis of the modelled contribution of individual factors showed that K_S was the most important predictor of the variation in site mean ν_H along the elevation gradient (Fig. 3). With high K_S, plants had large leaf area, leading to low ν_H. In addition, χ played a crucial role in ν_H variation, as well as being included in the effect of m_C. The improvement in R^2 contributions for the relationships of predicted $\log_e(\nu_H)$ to contributions due to different predictors was 0.59 for K_S, 0.14 for D, 0.10 for χ, 0.09 for c_a, and 0.06 for V_{cmax} and 0.03 for Ψ_{tlp} (Fig. 3a); or in an alternative breakdown of controls, 0.42 for K_S, 0.21 for temperature, 0.17 for radiation, 0.10 for D, 0.06 for elevation and 0.03 for Ψ_{tlp} (Fig. 3b).

Discussion

The results of path analysis (Fig. 2) and the success of the optimality model (Fig. 4) are consistent with the proposed central role of ν_H in coordinating hydraulic and photosynthetic traits (Rosas *et al.*, 2019). The ν_H variation mainly results from that in K_S and χ or temperature. Species deploying a larger total leaf area at a given sapwood area (lower ν_H) tend to have higher K_S (Togashi *et al.*, 2015). The relatively rapid acclimation of photosynthetic traits to the local environment (Smith & Dukes, 2017) that leads to the indirect relationship between ν_H and χ (Fig. S2i) has been noted before (Martinez-Vilalta *et al.*, 2009). However,
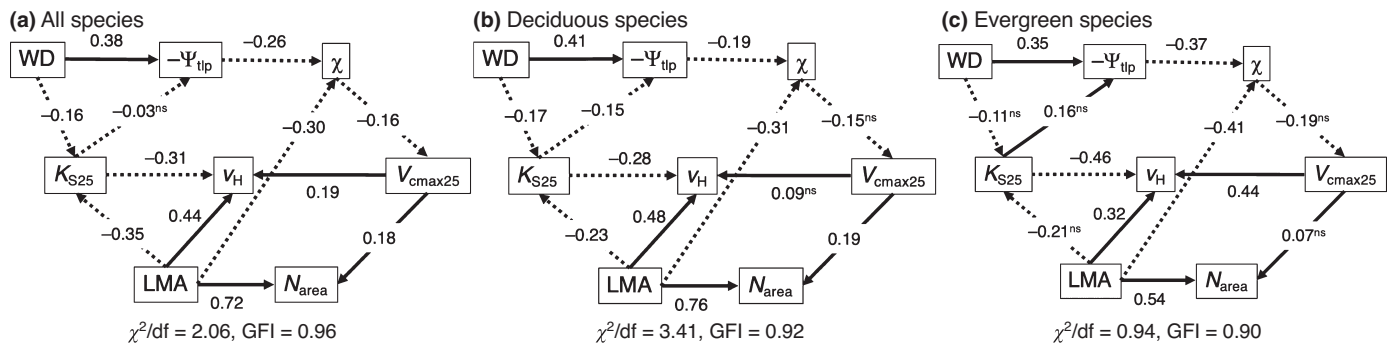
Fig. 2 Path analysis of hydraulic and photosynthetic traits for all species (a), separately deciduous (b) and evergreen species (c). WD is wood density, K_{S25} is sapwood-specific hydraulic conductivity at 25°C, Ψ_{tlp} is leaf water potential at turgor loss point, v_H is the ratio of sapwood to leaf area, LMA is leaf mass per area, χ is the ratio of leaf-internal to ambient CO_2 partial pressure, N_{area} is leaf nitrogen content per area, and V_{cmax25} is the maximum capacity of carboxylation at 25°C. The arrows indicate the proposed links between traits. Solid lines indicate positive relationships, dotted lines negative relationships. Standard path coefficients are shown near the line (ns, not significant). The trait coordination structure was evaluated using the ratio of χ^2 and degree of freedom (χ^2/df) and goodness-of-fit index (GFI).
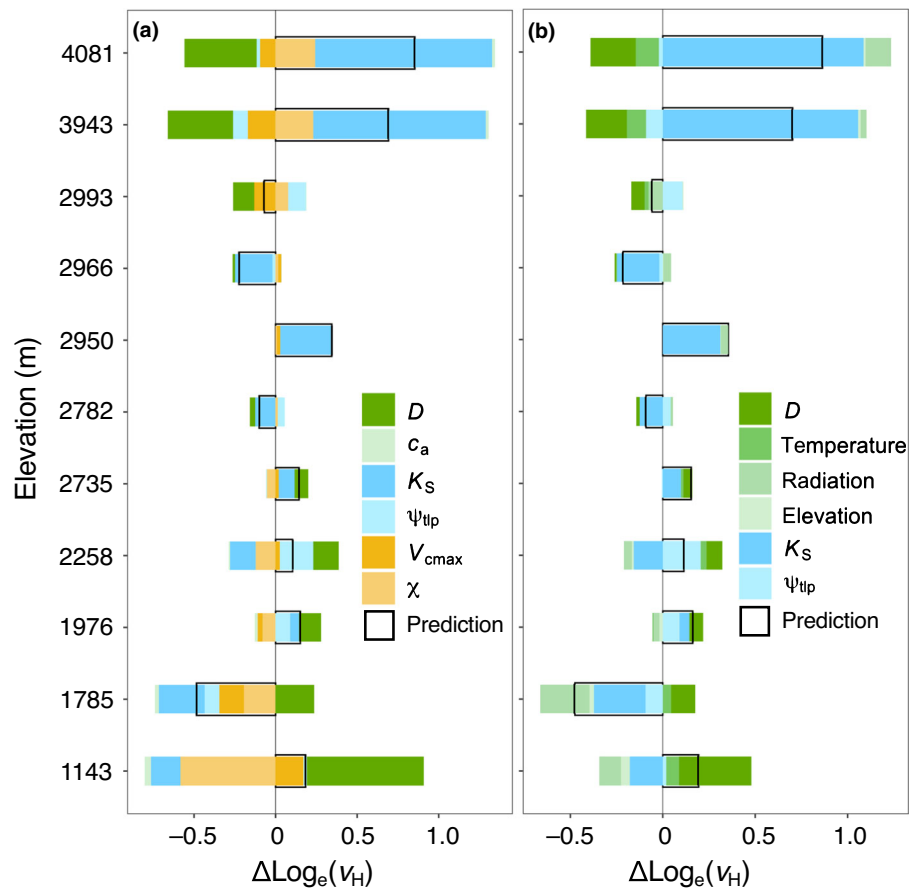

Fig. 3 The modelled contribution of different predictors to v_H variation at 11 sites sampled along an elevational gradient in the Gongga Mountains, China. (a) Contribution of direct predictors from Eqn 8. (b) Total contribution of environmental predictors through maximum capacity of carboxylation (V_{cmax}), the ratio of leaf-internal to ambient CO_2 partial pressure (χ) and c_a, along with hydraulic traits. In each panel, the vertical black line represents the baseline $\log_e(v_H)$ across sites (on which the data were centred, such that the x-axis represents the contribution of predictors: $\Delta\log_e(v_H)$). Transparent bars with black borders show the changes in predicted values compared with the baseline $\log_e(v_H)$. Environmental effects are shown in green; photosynthesis-related effects in orange; hydraulic trait effects: sapwood-specific hydraulic conductivity (K_S) and leaf water potential at turgor loss point (Ψ_{tlp}) are shown in blue.

the weak trade-off between Ψ_{tlp} and K_S in deciduous species and the apparent absence of these trade-offs in evergreen species imply that low hydraulic safety does not always accompany high K_S. Although the xylem tension at which 50% of the maximum conductivity is lost (P_{50}) is the most commonly used index of hydraulic safety, we used Ψ_{tlp} for this purpose, noting that the two measures are significantly correlated (Zhu et al., 2018; Joshi et al., 2020). Globally, a weak trade-off between hydraulic safety

and efficiency has been reported (Gleason et al., 2016), and new work suggests a tight trade-off between efficiency and safety may be a feature of climates with highly seasonal precipitation (Liu et al., 2021). That is, plants in environments with less seasonal precipitation need not have high hydraulic efficiency, which may be accompanied by unknown costs or risks.

The key role of v_H in mediating leaf physiology and hydraulics arises because of its relative plasticity. Variance partitioning (Fig. 1)
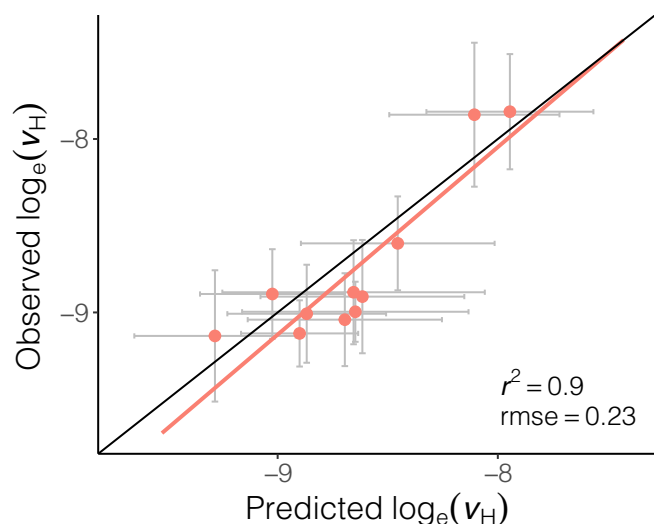
Fig. 4 Comparison between site mean observed and predicted ratios of sapwood to leaf area (v_H). The gray error bar in the y-axis direction is the standard deviation of observed $\log_e(v_H)$ at each site; that in the x-axis direction is the standard deviation of predictions, considering observed variations of sapwood-specific hydraulic conductivity (K_S) and leaf water potential at turgor loss point (Ψ_{tlp}).

showed that WD and K_S are far more strongly linked to phylogeny than other traits. This is presumably because both are related to wood anatomy. K_S is proportional to the fourth power of mean xylem conduit diameter (according to the Hagen–Poiseuille equation; Tyree & Ewers (1991)), while WD is largely dependent on fibre wall and lumen fractions (Ziemińska et al., 2013). Therefore, it might be expected that these traits would show a strong evolutionary convergence within lineages. By contrast, Ψ_{tlp} is known to change after drought through osmotic adjustment (Bartlett et al., 2014), implying a higher degree of plasticity consistent with the lower influence of family, and the higher influence of environmental factors, on this trait compared with other hydraulic traits (Fig. 1). The correlation between v_H and V_{cmax} provides the bridge between two sets of plant traits, resulting in the observed relationship between A_{sat} and hydraulic traits (Zhu et al., 2018; Deans et al., 2020). With higher V_{cmax}, leaves can fix more carbon, and stomata open to allow this action, entailing greater water loss. As photosynthetic traits, particularly χ and V_{cmax}, respond to environmental conditions on timescales of weeks to months by regulating intrinsic biochemical characteristics (Cavanagh & Kubien, 2014; Smith & Dukes, 2017), plants can adjust v_H relatively quickly by shedding leaves to balance water supply and demand (Choat et al., 2018), while potentially regulating K_S on a longer timescale. The acclimation timescales of different hydraulic traits lead to tight coordination with photosynthesis process. This coordination also avoids unnecessary carbon costs of hydraulic traits, and may help to ensure survival under unfavourable (drought) conditions. The prediction of v_H based on these essential trade-offs with observed hydraulic traits proves the intrinsic adjustment of hydraulic traits, implying that there is no need to try to predict hydraulic traits individually from climate alone. The key importance of this optimality model

is to successfully predict and unite the trade-offs among traits in an optimality framework.

WD has been considered as a crucial trait in a 'wood economics spectrum' linking water transport, mechanical support and tree mortality (Chave et al., 2009). Dense wood, found in many species from arid habitats, is generally associated with narrow conduits (Hacke & Sperry, 2001) that restrict hydraulic conductivity (Zanne et al., 2010) but also confers resistance to embolism (Anderegg et al., 2016), possibly due to thicker conduit walls and smaller pores in the pit membranes (Hacke et al., 2001; Pittermann et al., 2010). Wood xylem is the foundation for water transport; but leaves are often a major bottleneck for water flow, contributing 30% of whole-plant hydraulic resistance on average (Sack & Holbrook, 2006). Leaves with lower Ψ_{tlp} can keep their stomata open and continue photosynthesising at more negative water potentials; conversely, this strategy may incur a greater carbon cost to maintain leaf turgor (Bartlett et al., 2012; Deans et al., 2020; Sapes et al., 2021).

The tight relationships among LMA, v_H and K_S indicate biologically important interactions between carbon investment strategy and hydraulics. Leaves with low LMA tend to display a larger leaf area to fix carbon within a relatively short leaf life span. In addition, high hydraulic conductivity at both leaf and stem levels ensures that large amounts of water can be transported to leaves for transpiration, to maintain open stomata and a high rate of CO_2 uptake (Mencuccini et al., 2019b; Joshi et al., 2020). This relationship between hydraulics and LMA may also be associated with physiological characteristics. Thicker leaves (high LMA) tend to have a longer diffusional pathways in the mesophyll, which increases water movement resistance outside leaf xylem and decreases hydraulic conductivity (Flexas et al., 2013). The relationships between WD and K_S, and between LMA and K_S, for evergreen species were nonsignificant, possibly due to the relatively small sample size. Nonetheless, the fitted coefficients had the same sign and were of similar magnitude to those found for deciduous species. The reason for the weak relationship between v_H and V_{cmax} for deciduous species is unclear; again, the sign of the relationship was the same as that for the evergreen species.

The theory predicts direct impacts of vapour pressure deficit (D), and indirect effects of temperature, elevation and radiation, on v_H mediated by photosynthetic traits. As D increases, plants shed leaves and allocate more carbon to the root to reduce transpiration and absorb more water, leading to increasing v_H to balance water supply and demand (Trugman et al., 2019b). High D also causes reductions in gross primary production, and tree mortality (Park Williams et al., 2012; Yuan et al., 2019). Other environmental variables, including temperature and elevation, mainly influence hydraulic traits through their coordination with photosynthetic traits, which has been less examined in the field. The theory predicts a small positive impact of elevation on v_H, consistent with the occurrence of small-leaved species at high elevations (Wright et al., 2017) and the observed negative relationship between leaf size and v_H (Mencuccini et al., 2019b). Temperature has multiple competing effects that can be hard to disentangle, but the optimality model predicts an overall negative effect on v_H. Under future scenarios where both D and temperature are

projected to increase (Grossiord *et al.*, 2020), the optimality model offers a way to explore the potential v_H response as the net effect of several competing effects.

The prediction of site mean v_H using optimality theory offers a promising approach to implement hydraulics into vegetation and land-surface models. Although hydraulic processes are incorporated into some vegetation models to constrain photosynthesis, parameterisation of hydraulic traits such as v_H is required (Christoffersen *et al.*, 2016; Eller *et al.*, 2020). If the focus is on 'typical' vegetation in a given climate, the relationship we have predicted (and demonstrated) that applies to site mean v_H (Eqn 8), with photosynthetic traits predicted by optimality theory, could provide a straightforward way to couple photosynthetic and hydraulic traits in models. The prediction is much stronger for site means than for individual species – not surprisingly because the micro-environmental conditions to which each species acclimates are not known, while most current model applications are concerned only with the aggregate properties of the community.

The Huber value also reflects carbon allocation to leaf and biomass, which further affects productivity. A fixed parameter is used to partition carbon into leaf and stem in many vegetation models (Trugman *et al.*, 2019a). With the optimality model, the fixed parameter could be replaced by acclimated variation in v_H, leading to improved realism. However, there is considerable diversity in hydraulic traits (notably K_S) that is linked to LMA, which raises two practical issues if we are concerned with functional diversity: first, how to predict environmental influences on the leaf economics spectrum; second, how to deal with the large within-community variation in both LMA and K_S. Xu *et al.* (2021) have demonstrated a method to predict optimal LMA for deciduous plants, and a different approach is applicable to evergreen plants (Wang *et al.*, 2021). A way needs to be found to simultaneously estimate the *distribution* of values for highly variable, nonplastic traits. A solution to this problem would be a major step forward for modelling the terrestrial carbon, water and nitrogen cycles.

Acknowledgements

Author contributions

HX carried out the analyses and prepared the manuscript with contributions from all co-authors. HW, SPH and ICP designed the fieldwork, collected samples and measured plant traits. ICP and IJW developed and extended the least-cost theory. All authors contributed to the interpretation of the results.

ORCID

Sandy P. Harrison https://orcid.org/0000-0001-5687-1903
I. Colin Prentice https://orcid.org/0000-0002-1296-6764
Han Wang https://orcid.org/0000-0003-2482-1818
Ian J. Wright https://orcid.org/0000-0001-8338-9143
Huiying Xu https://orcid.org/0000-0003-3902-9620

Data availability

The trait data are presented in Table S2.

References

Anderegg WR, Klein T, Bartlett M, Sack L, Pellegrini AF, Choat B, Jansen S. 2016. Meta-analysis reveals that hydraulic traits explain cross-species patterns of drought-induced tree mortality across the globe. *Proceedings of the National Academy of Sciences, USA* **113**: 5024–5029.

Bartlett MK, Scoffoni C, Ardy R, Zhang Y, Sun S, Cao K, Sack L. 2012. Rapid determination of comparative drought tolerance traits: using an osmometer to predict turgor loss point. *Methods in Ecology and Evolution* **3**: 880–888.

Bartlett MK, Zhang Y, Kreidler N, Sun S, Ardy R, Cao K, Sack L. 2014. Global analysis of plasticity in turgor loss point, a key drought tolerance trait. *Ecology Letters* **17**: 1580–1590.

Bernacchi CJ, Singsaas EL, Pimentel C, Portis AR Jr, Long SP. 2001. Improved temperature response functions for models of Rubisco-limited photosynthesis. *Plant, Cell & Environment* **24**: 253–259.

Breheny P, Burchett W. 2017. Visualization of regression models using visreg. *R Journal* **9**: 56–71.

Brodribb TJ. 2009. Xylem hydraulic physiology: the functional backbone of terrestrial plant productivity. *Plant Science* **177**: 245–251.

Brodribb TJ, Feild TS, Jordan GJ. 2007. Leaf maximum photosynthetic rate and venation are linked by hydraulics. *Plant Physiology* **144**: 1890–1898.

Cavanagh AP, Kubien DS. 2014. Can phenotypic plasticity in Rubisco performance contribute to photosynthetic acclimation? *Photosynthesis Research* **119**: 203–214.

Cernusak LA, Ubierna N, Winter K, Holtum JA, Marshall JD, Farquhar GD. 2013. Environmental and physiological determinants of carbon isotope discrimination in terrestrial plants. *New Phytologist* **200**: 950–965.

Chave J, Coomes D, Jansen S, Lewis SL, Swenson NG, Zanne AE. 2009. Towards a worldwide wood economics spectrum. *Ecology Letters* **12**: 351–366.

Chen J-L, Reynolds JF, Harley PC, Tenhunen JD. 1993. Coordination theory of leaf nitrogen distribution in a canopy. *Oecologia* **93**: 63–69.

Choat B, Brodribb TJ, Brodersen CR, Duursma RA, López R, Medlyn BE. 2018. Triggers of tree mortality under drought. *Nature* **558**: 531–539.

Christoffersen BO, Gloor M, Fauset S, Fyllas NM, Galbraith DR, Baker TR, Kruijt B, Rowland L, Fisher RA, Binks OJ *et al.* 2016. Linking hydraulic

traits to tropical forest function in a size-structured and trait-driven model (TFS vol 1-Hydro). *Geoscientific Model Development* 9: 4227–4255.

Cornelissen JHC, Lavorel S, Garnier E, Díaz S, Buchmann N, Gurvich DE, Reich PB, Steege HT, Morgan HD, Heijden MGAVD *et al.* 2003. A handbook of protocols for standardised and easy measurement of plant functional traits worldwide. *Australian Journal of Botany* 51: 335–380.

Cornwell WK, Wright IJ, Turner J, Maire V, Barbour MM, Cernusak LA, Dawson T, Ellsworth D, Farquhar GD, Griffiths H *et al.* 2018. Climate and soils together regulate photosynthetic carbon isotope discrimination within C_3 plants worldwide. *Global Ecology and Biogeography* 27: 1056–1067.

Davis TW, Prentice IC, Stocker BD, Thomas RT, Whitley RJ, Wang H, Evans BJ, Gallego-Sala AV, Sykes MT, Cramer W. 2017. Simple process-led algorithms for simulating habitats (SPLASH vol 1.0): robust indices of radiation, evapotranspiration and plant-available moisture. *Geoscientific Model Development* 10: 689–708.

De Kauwe MG, Kala J, Lin YS, Pitman AJ, Medlyn BE, Duursma RA, Abramowitz G, Wang YP, Miralles DG. 2015. A test of an optimal stomatal conductance scheme within the CABLE land surface model. *Geoscientific Model Development* 8: 431–452.

De Kauwe MG, Lin YS, Wright IJ, Medlyn BE, Crous KY, Ellsworth DS, Maire V, Prentice IC, Atkin OK, Rogers A *et al.* 2016. A test of the 'one-point method' for estimating maximum carboxylation capacity from field-measured, light-saturated photosynthesis. *New Phytologist* 210: 1130–1144.

Deans RM, Brodribb TJ, Busch FA, Farquhar GD. 2020. Optimization can provide the fundamental link between leaf photosynthesis, gas exchange and water relations. *Nature Plants* 6: 1116–1125.

Dong N, Prentice IC, Evans BJ, Caddy-Retalic S, Lowe AJ, Wright IJ. 2017. Leaf nitrogen from first principles: field evidence for adaptive variation with climate. *Biogeosciences* 14: 481–495.

Dong N, Prentice IC, Wright IJ, Evans BJ, Togashi HF, Caddy-Retalic S, McInerney FA, Sparrow B, Leitch E, Lowe AJ. 2020. Components of leaf-trait variation along environmental gradients. *New Phytologist* 228: 82–94.

Eller CB, Rowland L, Mencuccini M, Rosas T, Williams K, Harper A, Medlyn BE, Wagner Y, Klein T, Teodoro GS *et al.* 2020. Stomatal optimization based on xylem hydraulics (SOX) improves land surface model simulation of vegetation responses to climate. *New Phytologist* 226: 1622–1637.

Farquhar GD, Ehleringer JR, Hubick KT. 1989. Carbon isotope discrimination and photosynthesis. *Annual Review of Plant Biology* 40: 503–537.

Farquhar GD, von Caemmerer S, Berry JA. 1980. A biochemical model of photosynthetic CO_2 assimilation in leaves of C_3 species. *Planta* 149: 78–90.

Fick A. 1855. Ueber diffusion. *Annalen der Physik* 170: 59–86.

Flexas J, Scoffoni C, Gago J, Sack L. 2013. Leaf mesophyll conductance and leaf hydraulic conductance: an introduction to their measurement and coordination. *Journal of Experimental Botany* 64: 3965–3981.

Franklin O, Harrison SP, Dewar R, Farrior CE, Brännström Å, Dieckmann U, Pietsch S, Falster D, Cramer W, Loreau M *et al.* 2020. Organizing principles for vegetation dynamics. *Nature Plants* 6: 444–453.

Gleason SM, Butler DW, Waryszak P. 2013. Shifts in leaf and stem hydraulic traits across aridity gradients in Eastern Australia. *International Journal of Plant Sciences* 174: 1292–1301.

Gleason SM, Westoby M, Jansen S, Choat B, Hacke UG, Pratt RB, Bhaskar R, Brodribb TJ, Bucci SJ, Cao K-F *et al.* 2016. Weak tradeoff between xylem safety and xylem-specific hydraulic efficiency across the world's woody plant species. *New Phytologist* 209: 123–136.

Groemping U. 2006. Relative importance for linear regression in R: the package relaimpo. *Journal of statistical software* 17: 925–933.

Grossiord C, Buckley TN, Cernusak LA, Novick KA, Poulter B, Siegwolf RTW, Sperry JS, McDowell NG. 2020. Plant responses to rising vapor pressure deficit. *New Phytologist* 226: 1550–1566.

Hacke UG, Sperry JS. 2001. Functional and ecological xylem anatomy. *Perspectives in Plant Ecology, Evolution and Systematics* 4: 97–115.

Hacke UG, Sperry JS, Pockman WT, Davis SD, McCulloh KA. 2001. Trends in wood density and structure are linked to prevention of xylem implosion by negative pressure. *Oecologia* 126: 457–461.

Hochberg U, Rockwell FE, Holbrook NM, Cochard H. 2018. Iso/anisohydry: a plant–environment interaction rather than a simple hydraulic trait. *Trends in Plant Science* 23: 112–120.

Hutchinson MF, Xu T. 2004. Anusplin version 4.2 user guide. *Centre for Resource and Environmental Studies, The Australian National University, Canberra* 54.

Joshi J, Stocker BD, Hofhansl F, Zhou S, Dieckmann U, Prentice IC. 2020. Towards a unified theory of plant photosynthesis and hydraulics. *bioRxiv* doi: 10.1101/2020.12.2017.423132.

Lavergne A, Sandoval D, Hare VJ, Graven H, Prentice IC. 2020a. Impacts of soil water stress on the acclimated stomatal limitation of photosynthesis: insights from stable carbon isotope data. *Global Change Biology* 26: 7158–7172.

Lavergne A, Voelker S, Csank A, Graven H, Boer HJ, Daux V, Robertson I, Dorado-Liñán I, Martínez-Sancho E, Battipaglia G *et al.* 2020b. Historical changes in the stomatal limitation of photosynthesis: empirical support for an optimality principle. *New Phytologist* 225: 2484–2497.

Liu H, Gleason SM, Hao G, Hua L, He P, Goldstein G, Ye Q. 2019. Hydraulic traits are coordinated with maximum plant height at the global scale. *Science Advances* 5: eaav1332.

Liu H, Ye Q, Gleason SM, He P, Yin D. 2021. Weak tradeoff between xylem hydraulic efficiency and safety: climatic seasonality matters. *New Phytologist* 229: 1440–1452.

Martínez-Vilalta J, Cochard H, Mencuccini M, Sterck F, Herrero A, Korhonen J, Llorens P, Nikinmaa E, Nolè A, Poyatos R *et al.* 2009. Hydraulic adjustment of Scots pine across Europe. *New Phytologist* 184: 353–364.

Mencuccini M, Manzoni S, Christoffersen B. 2019a. Modelling water fluxes in plants: from tissues to biosphere. *New Phytologist* 222: 1207–1222.

Mencuccini M, Rosas T, Rowland L, Choat B, Cornelissen H, Jansen S, Kramer K, Lapenis A, Manzoni S, Niinemets Ü *et al.* 2019b. Leaf economics and plant hydraulics drive leaf : wood area ratios. *New Phytologist* 224: 1544–1556.

Oksanen J, Blanchet FG, Friendly M, Kindt R, Legendre P, McGlinn D, Minchin PR, Ohara R, Simpson GL, Solymos P *et al.* 2017. vegan: Community Ecology Package. R package v.2.4-4 2: 1–295.

Olson ME, Anfodillo T, Gleason SM, McCulloh KA. 2021. Tip-to-base xylem conduit widening as an adaptation: causes, consequences, and empirical priorities. *New Phytologist* 229: 1877–1893.

Park Williams A, Allen CD, Macalady AK, Griffin D, Woodhouse CA, Meko DM, Swetnam TW, Rauscher SA, Seager R, Grissino-Mayer HD *et al.* 2012. Temperature as a potent driver of regional forest drought stress and tree mortality. *Nature Climate Change* 3: 292–297.

Pittermann J, Choat B, Jansen S, Stuart SA, Lynn L, Dawson TE. 2010. The relationships between xylem safety and hydraulic efficiency in the Cupressaceae: the evolution of pit membrane form and function. *Plant Physiology* 153: 1919–1931.

Poorter H, Niinemets U, Poorter L, Wright IJ, Villar R. 2009. Causes and consequences of variation in leaf mass per area (LMA): a meta-analysis. *New Phytologist* 182: 565–588.

Prentice IC, Dong N, Gleason SM, Maire V, Wright IJ. 2014. Balancing the costs of carbon gain and water transport: testing a new theoretical framework for plant functional ecology. *Ecology Letters* 17: 82–91.

R Core Team. 2015. *R: a language and environment for statistical computing.* Vienna, Austria: R Foundation for Statistical Computing. R v.3.1.3. [WWW document] URL https://www.r-project.org/ [accessed 16 July 2019].

Rosas T, Mencuccini M, Barba J, Cochard H, Saura-Mas S, Martinez-Vilalta J. 2019. Adjustments and coordination of hydraulic, leaf and stem traits along a water availability gradient. *New Phytologist* 223: 632–646.

Rosseel Y. 2012. Lavaan: An R package for structural equation modeling and more. Version 0.5–12 (BETA). *Journal of Statistical Software* 48: 1–36.

Rowland L, da Costa ACL, Galbraith DR, Oliveira RS, Binks OJ, Oliveira AAR, Pullen AM, Doughty CE, Metcalfe DB, Vasconcelos SS *et al.* 2015. Death from drought in tropical forests is triggered by hydraulics not carbon starvation. *Nature* 528: 119–122.

Sack L, Holbrook NM. 2006. Leaf hydraulics. *Annual Review of Plant Biology* 57: 361–381.

Santiago LS, Goldstein G, Meinzer FC, Fisher JB, Machado K, Woodruff D, Jones T. 2004. Leaf photosynthetic traits scale with hydraulic conductivity and wood density in Panamanian forest canopy trees. *Oecologia* 140: 543–550.

Sapes G, Demaree P, Lekberg Y, Sala A. 2021. Plant carbohydrate depletion impairs water relations and spreads via ectomycorrhizal networks. *New Phytologist* 229: 3172–3183.

Scoffoni C, Chatelet DS, Pasquet-Kok J, Rawls M, Donoghue MJ, Edwards EJ, Sack L. 2016. Hydraulic basis for the evolution of photosynthetic productivity. *Nature Plants* 2: 16072.

Smith NG, Dukes JS. 2017. Short-term acclimation to warmer temperatures accelerates leaf carbon exchange processes across plant types. *Global Change Biology* 13: 4840–4853.

Smith NG, Keenan TF, Colin Prentice I, Wang H, Wright IJ, Niinemets Ü, Crous KY, Domingues TF, Guerrieri R, Yoko Ishida F *et al.* 2019. Global photosynthetic capacity is optimized to the environment. *Ecology Letters* 22: 506–517.

Sperry JS, Donnelly JR, Tyree MT. 1988. A method for measuring hydraulic conductivity and embolism in xylem. *Plant, Cell & Environment* 11: 35–40.

Sperry JS, Venturas MD, Anderegg WRL, Mencuccini M, Mackay DS, Wang Y, Love DM. 2017. Predicting stomatal responses to the environment from the optimization of photosynthetic gain and hydraulic cost. *Plant, Cell & Environment* 40: 816–830.

Togashi HF, Prentice IC, Evans BJ, Forrester DI, Drake P, Feikema P, Brooksbank K, Eamus D, Taylor D. 2015. Morphological and moisture availability controls of the leaf area-to-sapwood area ratio: analysis of measurements on Australian trees. *Ecology and Evolution* 5: 1263–1270.

Trugman AT, Anderegg LDL, Sperry JS, Wang Y, Venturas M, Anderegg WRL. 2019a. Leveraging plant hydraulics to yield predictive and dynamic plant leaf allocation in vegetation models with climate change. *Global Change Biology* 25: 4008–4021.

Trugman AT, Anderegg LDL, Wolfe BT, Birami B, Ruehr NK, Detto M, Bartlett MK, Anderegg WRL. 2019b. Climate and plant trait strategies determine tree carbon allocation to leaves and mediate future forest productivity. *Global Change Biology* 25: 3395–3405.

Tyree MT, Ewers FW. 1991. The hydraulic architecture of trees and other woody plants. *New Phytologist* 119: 345–360.

Vogel H. 1921. Temperaturabhängigkeitsgesetz der Viskosität von Flüssigkeiten. *Physik Z* 22: 645–646.

Wang H, Colin Prentice I, Wright IJ, Qiao S, Xu X, Kikuzawa K, Stenseth NC. 2021. Leaf economics explained by optimality principles. *bioRxiv*. doi: 10.1101/2021.02.07.430028.

Wang H, Prentice IC, Keenan TF, Davis TW, Wright IJ, Cornwell WK, Evans BJ, Peng C. 2017. Towards a universal model for carbon dioxide uptake by plants. *Nature Plants* 3: 734–741.

Whitehead D. 1998. Regulation of stomatal conductance and transpiration in forest canopies. *Tree Physiology* 18: 633–644.

Wright IJ, Dong N, Maire V, Prentice IC, Westoby M, Díaz S, Gallagher RV, Jacobs BF, Kooyman R, Law EA *et al.* 2017. Global climatic drivers of leaf size. *Science* 357: 917–921.

Wright IJ, Reich PB, Westoby M, Ackerly DD, Baruch Z, Bongers F, Cavender-Bares J, Chapin T, Cornelissen JHC, Diemer M *et al.* 2004. The worldwide leaf economics spectrum. *Nature* 428: 821.

Xu H, Wang H, Prentice IC, Harrison SP, Wang G, Sun X. 2021. Predictability of leaf traits with climate and elevation: a case study in Gongga Mountain, China. *Tree Physiology*. doi: 10.1093/treephys/tpab003.

Yuan W, Zheng Yi, Piao S, Ciais P, Lombardozzi D, Wang Y, Ryu Y, Chen G, Dong W, Hu Z *et al.* 2019. Increased atmospheric vapor pressure deficit reduces global vegetation growth. *Science Advances* 5: eaax1396.

Zanne AE, Westoby M, Falster DS, Ackerly DD, Loarie SR, Arnold SE, Coomes DA. 2010. Angiosperm wood structure: global patterns in vessel anatomy and their relation to wood density and potential conductivity. *American Journal of Botany* 97: 207–215.

Zhu SD, Chen YJ, Ye Q, He PC, Liu H, Li RH, Fu PL, Jiang GF, Cao KF. 2018. Leaf turgor loss point is correlated with drought tolerance and leaf carbon economics traits. *Tree Physiology* 38: 658–663.

Ziemińska K, Butler DW, Gleason SM, Wright IJ, Westoby M. 2013. Fibre wall and lumen fractions drive wood density variation across 24 Australian angiosperms. *AoB Plants* 5: plt046.

Supporting Information

Additional Supporting Information may be found online in the Supporting Information section at the end of the article.

Fig. S1 Locations of sampling sites and weather stations.

Fig. S2 Bivariate relationships between traits.

Fig. S3 Partial residual plots from the regression of $\log_e$ transformation of the ratio of sapwood to leaf area (v_H) against different predictors.

Fig. S4 Comparison between observed and predicted ratios of sapwood to leaf area (v_H) across species.

Table S1 Variance-covariance matrices of traits for deciduous and evergreen species.

Table S2 The trait data used in this study.

Please note: Wiley Blackwell are not responsible for the content or functionality of any Supporting Information supplied by the authors. Any queries (other than missing material) should be directed to the *New Phytologist* Central Office.